ARTICLE

Quantitative Control of Neuron Adhesion at a Neural Interface Using a Conducting Polymer Composite with Low Electrical Impedance

Sung Yeol Kim,[†] Kwang-Min Kim,[†] Diane Hoffman-Kim,[†,‡] Hyun-Kon Song,[§] and G. Tayhas R. Palmore*[,†,‡,∥]

School of Engineering, Department of Molecular Pharmacology, Physiology, and Biotechnology, and Department of Chemistry, Brown University, Providence, Rhode Island 02912, United States, and Interdisciplinary School of Green Energy & School of Nano-Biotechnology and Chemical Engineering, Ulsan National Institute of Science & Technology, Banyeon-ri 100, Ulju-gun, Ulsan 689-798, Korea

ABSTRACT Tailoring cell response on an electrode surface is essential in the application of neural interfaces. In this paper, a method of controlling neuron adhesion on the surface of an electrode was demonstrated using a conducting polymer composite as an electrode coating. The electrodeposited coating was functionalized further with biomolecules-of-interest (BOI), with their surface concentration controlled via repetition of carbodiimide chemistry. The result was an electrode surface that promoted localized adhesion of primary neurons, the density of which could be controlled quantitatively via changes in the number of layers of BOI added. Important to neural interfaces, it was found that additional layers of BOI caused an insignificant increase in the electrical impedance, especially when compared to the large drop in impedance upon coating of the electrode with the conducting polymer composite.

KEYWORDS: neural interface • conducting polymers • polypyrrole • electrochemical impedance • poly(L-lysine)

INTRODUCTION

Neural interfaces are engineered devices designed to link an electrical system to the nervous system. Interest in these devices has increased because they can be used to study sensory or motor impairments as well as treat neurological disorders such as Parkinson's disease and epilepsy (1−3). Other uses of neural interfaces include biosensors (4). The most important feature of the neural interface is the physical contact between the biological tissue and the electrode surface. An electrode surface should possess three characteristics before being considered for a neural interface: (i) biocompatibility, (ii) low electrical impedance (or resistance), and (iii) long-term stability.

Biocompatibility is achieved by coating the surface of the electrode with a biomimetic material that ensures good viability of attached neurons (i.e., by promoting cell adhesion, proliferation, and neurite extension). In addition, the biomimetic material should not stimulate an inflammatory response or the formation of scar tissue. Strong and specific cell adhesion and neurite growth on a surface will enhance the communication between biological and electrical systems only if the surface coating used to enhance the biocompatibility is electrically conductive. A surface coating with high electrical impedance will hinder the flow of charge between neurons and electrodes, reducing the signal intensity during recording or stimulation because of a large *IR* drop (i.e., below the action potential). Different materials such as noble metals and metal oxides have been used as the interfacing material (5, 6). Recently, conducting polymers, such as polypyrrole (pPy) and poly(3,4-ethylenedioxythiophene), have been considered to be good candidates for supporting matrices used in nerve regeneration (7) and for electrode coatings used in neural interfaces (8, 9).

Polypyrrole satisfies *passive* biocompatibility (10); that is, an adverse tissue response is not observed at implants coated with this material, while simultaneously this material exhibits low electrical impedance (9). Several strategies have been developed to enhance the biocompatibility of pPy (i.e., *active* biocompatibility) via the codeposition of biomolecules or related compounds with pPy (11−13). Other strategies involve phage display (14) or monomers with reactive functional groups (15, 16). In our previous work, we developed a strategy where biomolecules-of-interest (BOI) were attached to functional groups of poly(glutamic acid) (pGlu) doped in pPy (17). Attachment of BOI to pPy[pGlu] occurs via the reaction of amine groups of the incoming BOI (e.g., *x*) with activated carboxylate groups of pGlu that protrude from the surface of pPy[pGlu]. This strategy ensures that most BOI are confined to the surface of the coating (pPy-[pGlu]-*x*) and are thus available as cues for adherent cells.

All of the strategies described above can be classified as strategies that focus solely on the *spatial* control of neuron adhesion and neurite extension within a defined area by providing a biocompatible surface with a fixed concentration

* Corresponding author. E-mail: Tayhas_Palmore@brown.edu.
Received for review March 29, 2010 and accepted November 11, 2010
† School of Engineering, Brown University.
‡ Department of Molecular Pharmacology, Physiology, and Biotechnology, Brown University.
∥ Department of Chemistry, Brown University.
§ Ulsan National Institute of Science & Technology.
DOI: 10.1021/am1008369

Published on Web 12/13/2010

of BOI. In addition to spatial control, strategies are needed that quantitatively control the concentration of BOI at a surface. This need arises from the fact that the extent of interaction between cells and electrodes can be adjusted by varying the concentration of BOI on the surface of conducting substrates such as pPy because many important cellular processes (e.g., adhesion, proliferation, differentiation, motility, and apoptosis) are affected by the concentration of BOI on the surface to which cells are in contact (18−22). Only a few studies, however, have demonstrated quantitative control over the concentration of BOI on the surface of pPy (16, 23, 24). Moreover, in the context of neural interfaces, the effect of the BOI concentration on the impedance of the underlying conductive substrate has not been studied previously.

In this work, the utility of (pPy[pGlu]-*x*) from our previous study is expanded to include control over the surface concentration of BOI via the sequential addition of layers of BOI to the surface of an electrode. This expanded utility results in biocompatible surfaces with which one can control *both* the location and density of the neurons and their neural processes adhered to an electrode surface. Importantly, electrodes coated in this manner exhibit a significant drop in the electrical impedance when compared to bare electrodes or electrodes coated with physisorbed films of BOI.

EXPERIMENTAL SECTION

Synthesis of pPy[pGlu]-pLys$_n$. Patterned polymer composite films were prepared using the previously reported procedure (17). Briefly, pPy doped with pGlu was electrodeposited from a solution containing 0.2 M pyrrole and 2 mM pGlu (based on the monomeric unit of glutamic acid) onto a glass slide coated with either indium−tin oxide (ITO; for cell culture and optical microscopy) or gold [for Fourier transform infrared (FTIR) measurements]. The thickness and sheet resistance of the ITO-coated glass were 100 nm and 20 Ω/sq, respectively. A fraction of pGlu protruding from the surface of pPy[pGlu] provides carboxylic acid groups, to which poly(L-lysine) (pLys) is coupled via 1-ethyl-3-[3-(dimethylamino)propyl]carbodiimide hydrochloride/*N*-hydroxysuccinimide (EDC/NHS) coupling reactions. Additional pLys layers are attached by repeating the EDC/NHS chemistry. The procedure for electrodeposition of pPy doped with both pGlu and Cl^- was the same as that described above except that 0.1 M KCl was added to the electrosynthesis solution.

Fibronectin (FN) Adsorption. FN (lyophilized from human plasma, Invitrogen) was reconstituted to 1 mg/mL in phosphate-buffered saline using Snake Skin pleated dialysis tubing (10 000 MWCO). All adsorption experiments were done for 2 h using solutions with a FN concentration of 0.1 mg/mL at 23 °C and pH 7.4, unless otherwise specified. FTIR spectroscopic studies were performed in the same manner as that described in the previous study except that gold-coated coverslips (18 × 18 mm^2) were used during the electrodeposition of pPy[pGlu] (17). The relative amount of adsorbed FN was determined from the difference in the intensity of the absorbance of the amide I peaks in the FTIR spectra of the samples before and after FN adsorption: $\Delta abs = abs\{pPy[pGlu]\text{-}pLys_n + FN\} - abs\{pPy[pGlu]\text{-}pLys_n\}$, where n is 0−3.

Impedance Measurements. Electrochemical impedance spectroscopy (Solartron 1255) coupled to a potentiostat (model 273A, EG&G Princeton Applied Research) was used to measure the impedance of a film of pPy[pGlu]-pLys$_n$ as a function of the frequency. The film was electrodeposited onto unpatterned ITO-coated glass with a surface area of 0.18 cm^2. The electrodes were equilibrated in 0.2 M KCl for at least 2 min at a direct-current (dc) bias potential of +100 mV vs Ag/AgCl. A 5 mV root-mean-square alternating-current amplitude with a frequency ranging from 1 Hz to 100 kHz was superimposed on the dc bias potential.

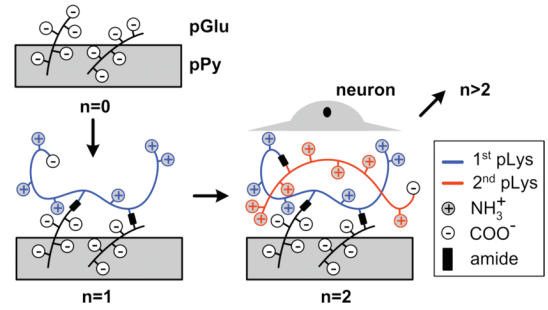

FIGURE 1. Schematic representation of a neuron adhered to a substrate consisting of pPy doped with pGlu and subsequently modified with multiple layers of pLys (pPy[pGlu]-pLys$_n$) via reaction with protruding carboxylic acid groups of the pGlu dopant.

Preparation of Hippocampal Neurons. Hippocampi (Fischer 344 rat, embryonic day 18; from BrainBits, LLC) were incubated in 0.25% trypsin in Hank's Balanced Salt Solution at 37 °C for 15 min. Digestion was terminated by removing trypsin and rinsing three times with Hank's Balanced Salt Solution at 37 °C for 5 min. The digested tissue was dissociated by trituration in Dulbecco's Modified Eagle Medium, 10% fetal bovine serum, 4 mM L-glutamine, and penicillin (100 U/mL)/streptomycin (100 mg/mL). Cells were added to substrates in a 24-well plate at a density of 30 000 cells/well and incubated in media with a serum at 37 °C and 5% CO_2 for 3 h. After plating, hippocampal neurons were cultured in a serum-free medium (neurobasal medium, 0.5 mM GlutaMAX, B27 supplement) at 37 °C and 5% CO_2. Control samples consisted of cells cultured on acid-washed glass coverslips coated with a 0.1% solution of pLys. The procedures of immunocytochemistry and optical analysis are described in our previous paper (17).

RESULTS AND DISCUSSION

Quantitative Control of the Surface Concentration of pLys. In our previous work, we demonstrated the use of pPy[pGlu]-pLys to control the spatial distribution of cells adhered to a surface (17). In this work, we advance the utility of this polymer composite to include control over the *density* of cells adhered to a surface. This control is exerted via the sequential addition of pLys layers to pPy[pGlu] for the purpose of changing the surface concentration of pLys. pLys was selected because it is a known biochemical cue that supports neuron adhesion and neurite outgrowth (25, 26). Shown in Figure 1 is our strategy for modulating the surface concentration of biomolecules on a pPy[pGlu]-coated electrode via sequential reactions that result in amide-bond formation. The polymer composite (pPy[pGlu]-pLys) is prepared first by electrodeposition of a conductive film of pPy[pGlu] onto a glass slide coated with ITO. A percentage of pGlu doped in pPy protrudes from the surface of pPy[pGlu], providing multiple chains of carboxylic acid groups that can be activated for the subsequent covalent attachment of pLys. First, a layer of pLys was attached to pPy[pGlu] ($n = 1$ in Figure 1) using EDC/NHS coupling chemistry, where a terminal carboxylate of pGlu incorporated into the pPy film

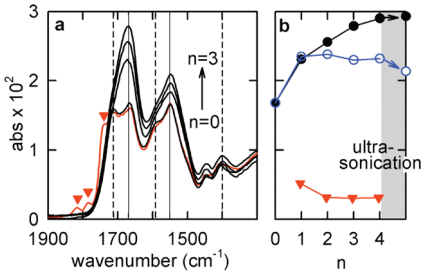

FIGURE 2. (a) IR spectra of pPy[pGlu] subsequent to activation by EDC/NHS (red line) and subsequent to reaction with pLys$_n$, where n = 0−3 (black lines), to yield pPy[pGlu]-pLys$_n$. (b) Intensity of the amide peak of pLys at 1675 cm^{-1} in part a as a function of n. Solid circles: pLys attached to pPy[Glu] via covalent bonds. Open circles: pLys attached to pPy[Glu] via physisorption. Included in part b are intensity data corresponding to the succinimide ester peak at 1740 cm^{-1} (red triangles) obtained by subtracting the intensity at 1740 cm^{-1} in spectra of pPy[pGlu]-pLys$_{n-1}$ from that of the same polymer activated with EDC/NHS (i.e., {pPy[pGlu]-pLys$_{n-1}$-NHS}−pPy[pGlu]-pLys$_{n-1}$, where n = 1−4).

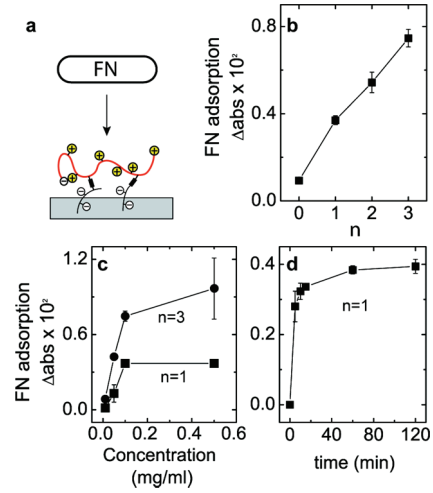

FIGURE 3. (a) Schematic representation of the adsorption of FN on pPy[pGlu]-pLys$_n$, where n = 1. Amount of FN adsorbed versus (b) the number of pLys layers (n), (c) concentration of FN in solution, and (d) adsorption time. Δabs was obtained by subtracting the intensity of the amide I peak (1675 cm^{-1}) of pPy[pGlu]-pLys$_n$, where n = 0−3 from the intensity of the amide I peak of the same substrate after adsorption of FN. An aqueous solution of FN (0.1 mg/mL) at pH 7.4 was used unless otherwise indicated.

reacts with an amino group of the incoming pLys. This reaction was repeated for additional layers of pLys (n = 2 and 3).

White light interferometry (WLI) and atomic force microscopy (AFM) were used to measure the thickness of dry samples of films of pPy[pGlu]-pLys$_n$ where n = 0−3 (see Figure S1 in the Supporting Information). The thickness of pPy[pGlu] is 10.4 ± 0.739 nm by WLI and 10.1 ± 1.98 nm by AFM. The average thickness of pPy[pGlu]-pLys$_n$ is 13.1 ± 1.16 nm by WLI and 14.8 ± 2.37 nm by AFM, regardless of the number of layers of pLys (i.e., n = 1−3). This result suggests that the layers of pLys spread rather than stack on the surface of pPy[pGlu]. This spreading may be attributed to attractive interactions between negatively charged pGlu and positively charged pLys (n = 2 in Figure 1).

FTIR spectroscopy was used to confirm the formation of multilayers of pLys. Shown in Figure 2a are the IR spectra of the polymer composite before and after each reaction that leads to its chemical modification with pLys. As expected, the FTIR spectrum of pPy[pGlu] (n = 0 in Figure 2a) contains peaks characteristic of carboxylate and amide groups (indicated by vertical dashed and solid lines, respectively, in Figure 2a). The carboxylates of pGlu that are not electrostatically bound to pPy (i.e., dangling) are activated with EDC to form the O-urea derivative, followed by stabilization with NHS to give the succinimide ester (red spectra in Figure 2a). The ester subsequently reacts with α-amino groups or lysine residues of incoming pLys to form an amide bond. The covalent attachment of pLys to activated pPy[pGlu] results in an increase in the intensity of the amide peaks and the disappearance of the peaks corresponding to the succinimide ester, indicating that the coupling reaction proceeded to completion. The intensity of the amide peaks also increases with each additional layer of pLys (black circles in Figure 2b).

The amount of pLys attached in each layer was determined from the intensity of the absorbance due to the succinimide ester, which is an indirect measure of the amount of carboxylate available for activation. As shown in Figure 2b, the intensity of the succinimide ester peak (red triangles) is highest for the first layer (n = 1). The intensity of this peak decreases to approximately a third of its original value in subsequent layers (n = 2−4). On the basis of these results, it appears that the ratio of pLys in the first layer relative to the second layer is 3:1, indicating that three activated carboxylates in the first layer ultimately bind to only one pLys unit to form the second layer. In subsequent layers, the ratio of pLys in incoming layers relative to the underlying layer is 1:1.

Also shown in Figure 2b is a plot of the intensity of the amide peak at 1675 cm^{-1} as a function of the layer number. This data demonstrate the degree of control made possible by pPy[pGlu] over the surface concentration of pLys. When the attachment was based on the formation of a covalent bond (solid circles), the intensity of the amide peak was proportional to the number of layers of pLys. In contrast, when the attachment was based on physisorption or electrostatic attraction (open circles), the intensity of the amide peak did not increase after the initial layer of pLys was physisorbed onto the pPy[pGlu] substrate.

Sonication experiments were performed to test the stability of the films. This type of experiment is an accelerated test of the long-term stability of the films (a requirement for neural interfaces). Films consisting of covalently attached pLys were found to be more stable than those with physisorbed pLys. This difference in stability is revealed by the lack of change in the intensity of the amide peak after pPy[pGlu]-pLys (4) was subjected to 24 h of sonication. In contrast, 31 % of physisorbed pLys was lost from the surface of pPy[pGlu] after sonication despite the strength of the electrostatic attraction between pPy[pGlu](−) and pLys(+).

In addition to using FTIR to confirm the formation of multilayers of pLys, the amount of pLys attached to pPy[pGlu]-pLys$_n$ for each value of n was measured indirectly by monitoring the adsorption of FN onto pPy[pGlu]-pLys$_n$. Shown in Figure 3a is a schematic representation illustrating

the adsorption of FN to pPy[pGlu]-pLys$_n$ where $n = 1$. The total positive charge on the surface of pPy[pGlu]-pLys$_n$ increases as n increases, which results in a stronger electrostatic interaction with negatively charged FN (pI = 5.60) at neutral pH. The data shown in Figure 3b suggests that the amount of FN adsorbed onto the surface of pPy[pGlu]-pLys$_n$ increases proportionally with increasing layers of pLys (n). Shown in Figure 3c is a plot of FN adsorption (measured as intensity data) as a function of the concentration of FN in the media (pH 7.4). The amount of protein adsorbed onto the polymer substrate reaches a plateau at around 0.1 mg/mL for both $n = 1$ and 3. The amount of adsorbed FN on pPy[pGlu]-pLys$_3$ is approximately twice as much as that on pPy[pGlu]-pLys$_1$ for all four concentrations tested. Shown in Figure 3d is a plot of FN adsorption as a function of time. The initial adsorption of FN is fast, with more than 80% of the available FN adsorbed within the first 10 min. Subsequently, the amount of adsorbed FN increases slowly to a saturation value in 2 h. These results demonstrate that the amount of FN adsorbed to the surface of pLys in pPy[pGlu]-pLys$_n$ is highly dependent on the number of layers of pLys.

Other biomolecules with carboxylate and amine groups (e.g., ECM proteins, synthesized peptides) also can be attached to pPy[pGlu] in a similar manner. For example, as shown in Figure S2 in the Supporting Information, pPy[pGlu]-pLys can be covalently modified with multilayers of laminin (Lmn) to give pPy[pGlu]-pLys-Lmn$_m$.

Quantitative Control of Cell Adhesion. Gridlike micropatterns of pPy[pGlu]-pLys$_n$ were prepared by exploiting a unique property of conductive polymers; that is, they are electrodeposited only at electroactive surfaces to which a voltage has been applied. The resulting micropatterned substrates were used to study the localized adhesion of primary hippocampal neurons. Very few neurons were observed to attach to either untreated ITO or ITO coated with pPy[pGlu]. In contrast, neurons were observed to preferentially adhere to the micropatterns of pPy[pGlu]-pLys$_n$ and exhibit well-developed neurites (Figure 4). Similar results were obtained for cortical neurons and dorsal root ganglia. In general, all types of neurons adhered to the micropatterns of pPy[pGlu]-pLys$_n$ were viable and exhibited good neurite extension.

More cells adhered to a substrate where one layer of pLys was covalently bound to pPy[pGlu] (350 cells/mm^2 for $n = 1$) than to pLys-coated coverslips (182 cells/mm^2) as the control substrate. However, the cell density observed on the first layer of pLys (350 cells/mm^2 for $n = 1$) accounts for only 23% of the total of number of cells seeded. A few cells and neurites adhered outside of the micropattern, but the majority of the remaining total number of cells did not attach to the substrate (Figure 4a). When the surface concentration of pLys was increased with each additional layer (e.g., from $n = 1$ to 3), the density of adhered hippocampal neurons and neurites was found to increase proportionally to the surface concentration of pLys (Figure 4f). In addition, the number of cells adhered to areas outside the patterns of pPy[pGlu]-pLys$_n$ decreased as the number of layers of pLys

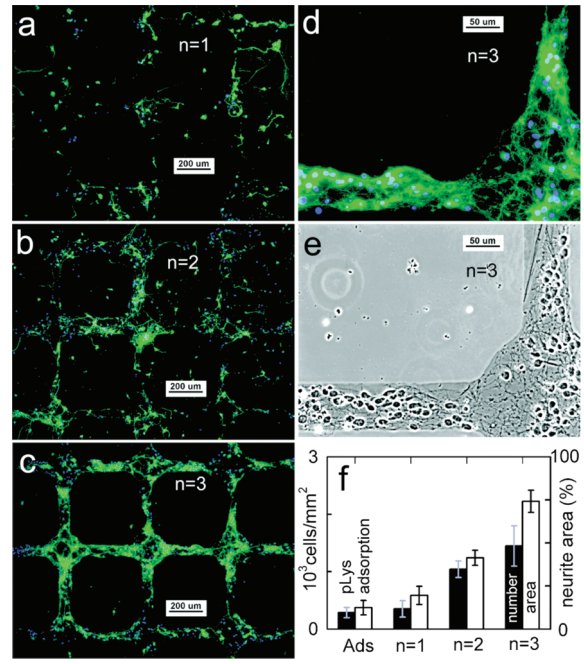

FIGURE 4. Immunofluorescent (a−d) and phase contrast (e) images of hippocampal neurons on pPy[pGlu]-pLys$_n$ 4 days after plating: the number of pLys layers is $n = 1$ (a), $n = 2$ (b), and $n = 3$ (c−e). Neurites stained positive for GAP-43 (green) and nuclei of all cells were labeled with DAPI (blue). (f) Number of cells adhered to patterns of pPy[pGlu]-pLys$_n$ (black bars) and area of pPy[pGlu]-pLys$_n$ covered by neurites (white bars). The increased density of adhered neurons and processes with n were statistically significant with $N = 4$ and $P < 0.001$ (ANOVA).

increased. Significantly, the density of the cells on the pPy[pGlu]-pLys$_n$ substrate where $n = 3$ (1447 cells/mm^2) approaches the maximum possible cell density if all cells plated adhered to the micropattern (1500 cells/mm^2). Neurites occupied over 70% of the micropattern of pPy[pGlu]-pLys$_3$. Although high concentrations of pLys have been reported to decrease the cell viability and number of neurites (27, 28), we did not observe these adverse effects. Thus, pPy[pGlu]-pLys$_n$ effectively controls both the spatial distribution of the adhered cells and their density.

A mixture of cells such as neurons, glial cells, astrocytes, and fibroblasts is found in nerve tissue. Neurobasal media/B27 without serum was used both to promote the growth of neurons and to suppress the growth of glial cells on coated electrodes during in vitro experiments (29). Because polylysine is not selective for neurons, however, in vivo applications would require the presence of cell adhesion molecules with neuron specificity such as IKVAV and YIGSR (30, 31). The concentration of these molecules is known to regulate cell adhesion (32, 33) and, thus, multilayer formation of IKVAV and YIGSR on pPy[pGlu] should be useful for optimizing the selective attachment of neurons in vivo.

Enhanced Electrical Property at the Interface. In addition to biocompatibility and stability (demonstrated in the previous sections), coatings used for neural interfaces should exhibit low electrical impedance or resistance. The frequency-dependent changes in impedance of ITO electrodes coated with pPy[pGlu]-pLys$_n$ were investigated and are shown as a Nyquist plot in Figure 5a. Both bare ITO and

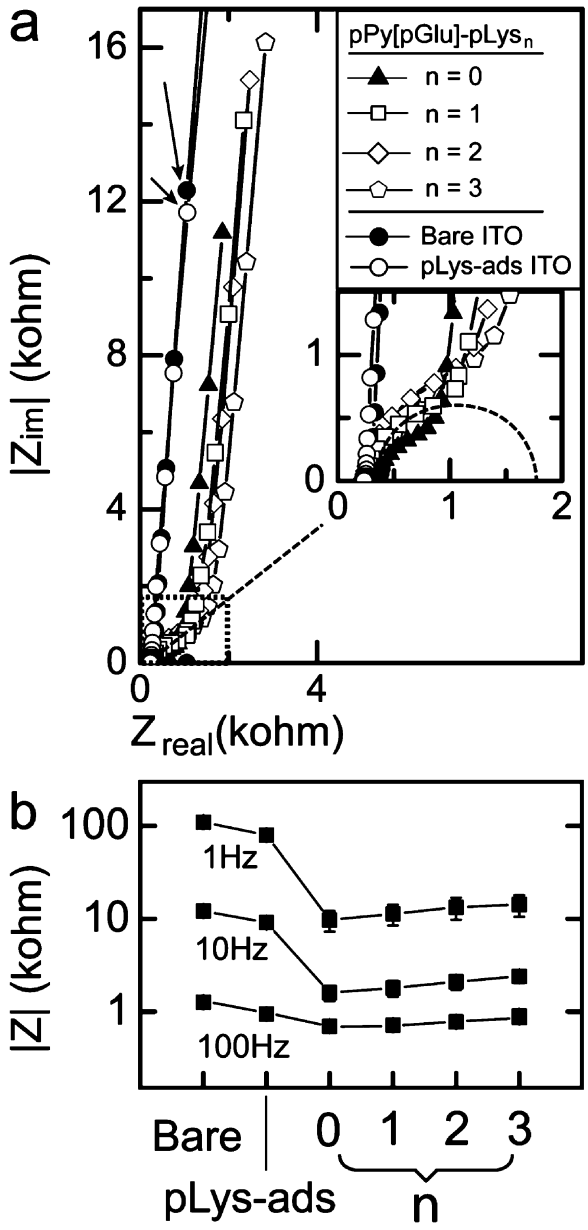

FIGURE 5. (a) Nyquist plots of bare, pLys-adsorbed, and pPy[pGlu]-pLys$_n$-coated ITO electrodes (legend shown in the figure): data with the highest value in the plots were obtained at 1 Hz for pPy[pGlu]-pLys$_n$-coated ITO electrodes and 6.3 Hz for bare and pLys-adsorbed ITO electrodes (indicated by arrows). High-frequency data within the dashed rectangle is enlarged in the inset. (b) Absolute total impedance ($|Z| = [(Z_{im})^2 + (Z_{real})^2]^{1/2}$) of ITO electrodes at selected frequencies (1, 10, and 100 Hz).

ITO with physisorbed pLys exhibit a straight line with a steep slope in their Nyquist plots, reflecting the impedance behavior of flat conductive surfaces. In comparison, ITO coated with pPy[pGlu]-pLys$_n$ ($n = 0-3$) exhibits the impedance behavior of a porous material based on two features of the Nyquist plot: firstly (1), the slope of the line at low frequencies is less steep than that of the uncoated or pLys-adsorbed ITO and secondly (2), the slope of the line at high frequencies is 45° (indicated by the dotted semicircle in Figure 5a, inset) in the high frequency range indicate electron transfer between different phases (e.g., from ITO to pPy or from one pPy particle or grain to another). A porous structure that provides a high specific surface area is beneficial in terms of cell or protein adhesion as well as interfacial impedance.

The absolute values of total impedance ($|Z|$) for the different electrodes were compared at selected frequencies (Figure 5b). Common to all electrodes studied, the absolute value of impedance decreases with increasing frequency because the capacitive element of impedance becomes small: at frequencies greater than 200 Hz, the impedance of the ITO electrodes is equivalent statistically (ANOVA, Holm-Sidak method; $P < 0.01$) regardless of whether the electrodes are coated with pPy[pGlu]-pLys$_n$ ($n = 0-3$) or uncoated. In contrast, the frequency dependence of $|Z|$ is different when coated and uncoated electrodes are compared over a frequency range of 1−200 Hz (neuron and cardiac myocyte signals generally occur in the range of 0.1−1000 Hz) (34). The ITO electrodes coated with pPy[pGlu]-pLys$_n$ ($n = 0-3$) exhibit a lower value of $|Z|$ compared to that of bare ITO or ITO coated with physisorbed pLys. The increase in the surface area originating from the porous structure of the polymer composite is responsible for the lower impedance at electrodes coated with pPy[pGlu]-pLys$_n$ (35). The large area of the interface provides more electrical pathways between adhered cells and the underlying electrode.

The impedance of ITO electrodes coated with pPy[pGlu]-pLys$_n$ was observed to increase incrementally with each additional layer of pLys (Figure 5b). This increase in the impedance, however, is insignificant relative to the decrease in the impedance upon coating an ITO electrode with pPy[pGlu]-pLys$_n$. For example, at low frequencies, the impedance decreases 10-fold (e.g., from 109 kΩ to 9.7 kΩ at 1 Hz) when a bare electrode is coated with pPy[pGlu]-pLys$_n$, while the subsequent addition of one layer of pLys to pPy[pGlu]-pLys$_n$ increases the impedance only slightly (e.g., 9.7 kΩ to 11.3 kΩ at 1 Hz). Thus, at low frequencies (1−200 Hz), the interfacial electrical properties of ITO electrodes are improved by coating the electrodes with pPy[pGlu]-pLys$_n$. Moreover, the surface concentration of pLys can be controlled by the number of layers (n of pPy[pGlu]-pLys$_n$) without significant adverse effects on the electrical properties of the electrode over the measured frequency range.

The mobile ions responsible for ionic transport within pPy[pGlu]-pLys$_n$ are cations because pPy is doped with a large anion (pGlu; molecular weight = 15 000−50 000). This mechanism of transport is similar to that observed in other conducting polymers doped with large anionic dopants such as poly(styrene sulfonate) (36). Thus, the small increase in the impedance caused by the additional layers of pLys is due, in part, to the fact that the addition of cationic pLys layers on top of pPy[pGlu] inhibits cation transport through the film. In contrast, a slight decrease in the impedance is observed at an ITO electrode coated with physisorbed pLys partly because the amount of charge on the surface of the ITO electrode has increased.

Interfacial impedance hinders communication between cells and electrodes. Coating electrodes with a conducting polymer has been reported to decrease the interfacial impedance. A 20−100-fold decrease in the impedance has

been reported in the frequency range of 1−1000 Hz depending on the thickness, surface roughness, and dopant of the conducting polymer film (37, 38). The thickness of the conducting polymer composite used in this work was about 10 nm (Figure S1 in the Supporting Information) and, therefore, the impedance data do not change at frequencies higher than 200 Hz. When an ITO electrode was coated with a thicker film of pPy doped with both pGlu and Cl anions (pPy[pGlu+Cl^-]), the impedance decreases 10−100-fold over the broader range of biologically relevant frequencies (i.e., 1−1000 Hz; Figure S3 in the Supporting Information).

CONCLUSION

In conclusion, this work demonstrates that the extent of cell adhesion and neurite extension at an electrode can be modulated by coating electrodes with a conductive polymer composite that has been modified with multilayers of a biomolecule of interest (pPy[pGlu]-$pLys_n$). These films were shown to be stable when subjected to ultrasonification, with a stability that exceeds physisorbed films of BOI. Importantly, pPy[pGlu]-$pLys_1$ was shown to decrease the electrical impedance of an ITO electrode by an order of magnitude, with additional layers of pLys only slightly increasing the impedance, while these additional layers of pLys significantly enhanced cell adhesion and neurite outgrowth on a target area.

Engineering a biomimetic environment on electrode surfaces is essential to realizing effective communication between adhered cells and the underlying electrode. This surface environment should promote strong interaction between the cells and the underlying electrode without degrading the electrical impedance of the electrode. This method of coating electrodes with conducting polymers functionalized with multilayers of BOI will be useful in biomedical applications, where the interface between a conductive surface and adhered cells must be strong with minimal electrical impedance.

Acknowledgment. This work was supported by the NSF, NIH, and NRF Korea (WCU/Basic).

Supporting Information Available: Thickness of pPy-[pGlu]-$pLys_n$, FTIR spectra of pPy[pGlu] modified with multilayers of Lmn, Bode plots of pPy[pGlu] and pPy[pGlu+Cl^-], and fluorescence assay of the surface concentration of pLys. This material is available free of charge via the Internet at http://pubs.acs.org.

REFERENCES AND NOTES

(1) Hambrecht, F. T. *Annu. Rev. Biophys. Bioeng.* **1979**, *8*, 239–267.
(2) Weiland, J. D.; Liu, W. T.; Humayun, M. S. *Annu. Rev. Biomed. Eng.* **2005**, *7*, 361–401.
(3) Schwartz, A. B. *Annu. Rev. Neurosci.* **2004**, *27*, 487–507.
(4) Pancrazio, J. J.; Whelan, J. P.; Borkholder, D. A.; Ma, W.; Stenger, D. A. *Ann. Biomed. Eng.* **1999**, *27*, 697–711.
(5) Brummer, S. B.; Robblee, L. S.; Hambrecht, F. T. *Ann. N.Y. Acad. Sci.* **1983**, *405*, 159–171.
(6) Cogan, S. F.; Troyk, P. R.; Ehrlich, J.; Plante, T. D. *IEEE Trans. Biomed. Eng.* **2005**, *52*, 1612–1614.
(7) Schmidt, C. E.; Shastri, V. R.; Vacanti, J. P.; Langer, R. *Proc. Natl. Acad. Sci. U.S.A.* **1997**, *94*, 8948–8953.
(8) Abidian, M. R.; Martin, D. C. *Adv. Funct. Mater.* **2009**, *19*, 573–585.
(9) Green, R. A.; Lovell, N. H.; Poole-Warren, L. A. *Biomaterials* **2009**, *30*, 3637–3644.
(10) Wang, X. D.; Gu, X. S.; Yuan, C. W.; Chen, S. J.; Zhang, P. Y.; Zhang, T.; Yao, Y. J.; Chen, F.; Chen, G. *J. Biomed. Mater. Res., Part A* **2004**, *68A*, 411–422.
(11) Garner, B.; Georgevich, A.; Hodgson, A. J.; Liu, L.; Wallace, G. G. *J. Biomed. Mater. Res.* **1999**, *44*, 121–129.
(12) Collier, J. H.; Camp, J. P.; Hudson, T. W.; Schmidt, C. E. *J. Biomed. Mater. Res.* **2000**, *50*, 574–584.
(13) Stauffer, W. R.; Cui, X. T. *Biomaterials* **2006**, *27*, 2405–2413.
(14) Sanghvi, A. B.; Miller, K. P. H.; Belcher, A. M.; Schmidt, C. E. *Nat. Mater.* **2005**, *4*, 496–502.
(15) Cosnier, S. *Biosens. Bioelectron.* **1999**, *14*, 443–456.
(16) Cen, L.; Neoh, K. G.; Kang, E. T. *Langmuir* **2002**, *18*, 8633–8640.
(17) Song, H. K.; Toste, B.; Ahmann, K.; Hoffman-Kim, D.; Palmore, G. T. R. *Biomaterials* **2006**, *27*, 473–484.
(18) Hansen, L. K.; Mooney, D. J.; Vacanti, J. P.; Ingber, D. E. *Mol. Biol. Cell* **1994**, *5*, 967–975.
(19) Mooney, D.; Hansen, L.; Vacanti, J.; Langer, R.; Farmer, S.; Ingber, D. *J. Cell Physiol.* **1992**, *151*, 497–505.
(20) Mooney, D. J.; Langer, R.; Ingber, D. E. *J. Cell Sci.* **1995**, *108*, 2311–2320.
(21) Palecek, S. P.; Loftus, J. C.; Ginsberg, M. H.; Lauffenburger, D. A.; Horwitz, A. F. *Nature* **1997**, *385*, 537–540.
(22) Carter, S. B. *Nature* **1967**, *213*, 256–260.
(23) Gomez, N.; Schmidt, C. E. *J. Biomed. Mater. Res., Part A* **2007**, *81A*, 135–149.
(24) Cosnier, S.; Galland, B.; Gondran, C.; Le Pellec, A. *Electroanalysis* **1998**, *10*, 808–813.
(25) Soekarno, A.; Lorn, B.; Hockberger, P. E. *Neuroimage* **1993**, *1*, 129–144.
(26) Jun, S. B.; Hynd, M. R.; Dowell-Mesfin, N. K.; Smith, L.; Turner, J. N.; Shain, W.; Kim, S. J. *J. Neurosci. Methods* **2007**, *160*, 317–326.
(27) Varon, S. *Neurochem. Res.* **1979**, *4*, 155–173.
(28) Crompton, K. E.; Goud, J. D.; Bellamkonda, R. V.; Gengenbach, T. R.; Finkelstein, D. I.; Horne, M. K.; Forsythe, J. S. *Biomaterials* **2007**, *28*, 441–449.
(29) Brewer, G. J.; Torricelli, J. R.; Evege, E. K.; Price, P. J. *J. Neurosci. Res.* **1993**, *35*, 567–576.
(30) Saneinejad, S.; Shoichet, M. S. *J. Biomed. Mater. Res.* **1998**, *42*, 13–19.
(31) Lu, S. Y.; Bansal, A.; Soussou, W.; Berger, T. W.; Madhukar, A. *Nano Lett.* **2006**, *6*, 1977–1981.
(32) Thid, D.; Holm, K.; Eriksson, P. S.; Ekeroth, J.; Kasemo, B.; Gold, J. *J. Biomed. Mater. Res., Part A* **2008**, *84A*, 940–953.
(33) Gunn, J. W.; Turner, S. D.; Mann, B. K. *J. Biomed. Mater. Res., Part A* **2005**, *72A*, 91–97.
(34) Stenger, D. A.; McKenna, T. M. *Enabling Technologies for Cultured Neural Networks*; Academic Press: New York, 1994.
(35) Cui, X. Y.; Lee, V. A.; Raphael, Y.; Wiler, J. A.; Hetke, J. F.; Anderson, D. J.; Martin, D. C. *J. Biomed. Mater. Res.* **2001**, *56*, 261–272.
(36) Bobacka, J. *Anal. Chem.* **1999**, *71*, 4932–4937.
(37) Kim, D. H.; Richardson-Burns, S. M.; Hendricks, J. L.; Sequera, C.; Martin, D. C. *Adv. Funct. Mater.* **2007**, *17*, 79–86.
(38) Keefer, E. W.; Botterman, B. R.; Romero, M. I.; Rossi, A. F.; Gross, G. W. *Nat. Nanotechnol.* **2008**, *3*, 434–439.

AM1008369